Morphology and Structure of Silica Agglomerates in Silica-Reinforced Silicone Rubber

A. V. GALANTI* and L. H. SPERLING,

Materials Research Center and Department of Chemical Engineering, Lehigh University, Bethlehem, Pennsylvania 18015

Synopsis

Light-scattering and optical microscope observations of silica-reinforced silicone rubber have shown that the filler is dispersed in a complex manner. Much of the original material appears agglomerated into particles several microns in size. These particles apparently further cluster to form agglomerates of about 20 μ in diameter. In an earlier paper in this series it was shown that the thermodynamic function f_e/f (the fraction of the retractive force due to internal energy changes) was a measure of the reinforcement level. It is now proposed that the corresponding physical mechanism of reinforcement may have its origin in the large amounts of energy required to deform the filler particle agglomerates.

INTRODUCTION

Silicone elastomers are commonly reinforced with finely divided silicas. These fillers increase the modulus, tensile strength, and swelling resistance of the material. In the previous papers in this series[1,2] a thermodynamic theory of reinforcement was developed. It was shown that forces arising from changes in internal energy, rather than changes in entropy, were primarily responsible for the reinforcement found in silica-filled silicone elastomers. The most likely physical mode of developing such internal energy changes involves deformation of agglomerates of the primary aggregates.[3] Other possible modes include bending of hydrogen bonds, crystallization or adsorption[4] of the polymer of the filler surface, or deformation of the primary filler particles.

The picture in the literature is complex. The BET[5] surface area of silica particles suitable for elastomer reinforcement is usually of the order of 150 m²/g.[6] The classic work of Bueche[7] suggested that on this basis one bond exists between the filler and the polymer for every 2 to 40 A^2 of area presented. Yet there appears to be only a general correlation between BET surface area and degree of reinforcement.[6,9] The objective of the present paper is to explore this problem employing optical microscopy and light-scattering techniques. These instruments permitted in situ studies

* Present address: The Hazleton Campus, The Pennsylvania State University, Hazleton, Pennsylvania 18201.

on the fully formulated reinforced elastomer. For comparison purposes, electron micrographs of the primary particles are also presented.

PARTICLE SURFACE AREA DETERMINATION VIA LIGHT SCATTERING

Light-scattering measurements can give useful information about non-homogeneous or two-phased systems if the characteristic dimensions of the particles are of the same order of magnitude as the wavelength of the radiation employed. Debye and Bueche[10] and later Debye, Anderson, and Brumberger[11] developed a method of determining the surface area S and the correlation distance a from the angular distribution of scattered radiation in such systems. The theory was first applied[16,11] to small-angle x-ray scattering experiments. However, theory and experiment were later broadened to include visible light-scattering studies.[12-16]

Experimentally, the parameter a is determined from a plot of $I_\theta^{-1/2}$ versus $4\sin^2(\theta/2)$ by the relation

$$a = \frac{\lambda'}{2\pi}\left(\frac{\text{slope}}{\text{intercept}}\right)^{1/2} \qquad (1)$$

where the wavelength of the light in the medium is λ' and I_θ is the intensity of the scattered light at angle θ.

Caulfield and Ullman[15,16] have shown that the original Debye correlation function $\gamma(r) = e^{-r/a}$, which was developed for irregular or randomly appearing surfaces, needed modification if the system had some structure. In particular, for dispersions of spheres, the particle radius R is given by

$$R^2 = 10a^2. \qquad (2)$$

A critical experimental prerequisite for Debye scattering is that the refractive index of the two phases nearly (but not exactly) match. The ratio of the refractive indices for the silica–silicone rubber system is 1.02, which satisfies this requirement.

EXPERIMENTAL

Materials

The silicone rubber–silica filler system employed has been described elswhere.[1,2] Briefly, four types of silicas, HiSil 233, Quso M-51, TK-302, and Celite (diatomaceous earth), listed in decreasing reinforcing efficiency, were milled into the linear polymer at various loadings. In addition to the normal cured elastomer, samples of the milled uncrosslinked composites were prepared in various thicknesses in the form of thin films supported between glass microscope slides. Special care was taken to exclude entrapped air bubbles.

Model systems of polystyrene lactices 1.8 μ in diameter, obtained from the Dow Chemical Company, were suspended in the silicone gum at various loadings. These were employed for comparative purposes.

Light-Scattering Photometer

A standard Brice-Phoenix photometer Model 2000 Series, manufactured by the Phoenix Instrument Company, was employed. All measurements were made with 5461 Å light. To allow scattering studies at the very low angles employed (2°–30° exterior angle), the beam was further collimated by placing a pinhole arrangement just before the sample. A special sample holder was constructed for the microscope slide–polymer sandwiches.

Several geometric and optical correction factors were employed[17,18] to obtain values of I_θ. These included attention to refraction and reflection effects at each interface, polarization of the scattered light, blank corrections, and secondary or multiple scattering.

The approach employed for the last-mentioned problem was to measure the scattered intensity as a function of sample thickness x and extrapolate plots of $(x/I_\theta)^{1/2}$ versus x to zero x. On the average, four thicknesses having transmissions from 70% to 95% were employed for each composite.

Microscopy

A transmission Carl Zeiss polarizing light microscope, Model GPL 668, equipped with a turret-mounted variable objective lens system ranging from $10\times$ to $100\times$ and an eye piece lens of $10\times$, was employed. Photomicrographs were taken with a 35-mm Exakta camera mounted on the microscope. Many of the glass slide–sample sandwiches prepared for the light-scattering studies were also appropriate for the microscopy study. Magnifications of $100\times$ and $630\times$ were employed for the silica-filled materials and polystyrene latices, respectively.

A full understanding of the nature of the filler–polymer interaction and the extent of aggregation requires an understanding of the nature of the primary filler particles. An RCA EMU 3-G electron microscope was employed. The samples were dispersed in an alcoholic solution with the aid of an ultrasonic vibrator and dried onto a carbon grid. No shadowing was required. Magnifications of ca. $55,000\times$ were studied.

EXPERIMENTAL RESULTS AND DISCUSSION

The Model System

Two dispersions of 1.8 μ polystyene latex spheres in silicone gum were studied. As shown in Figure 1, they differed primarily in their state of aggregation. Light-scattering studies on these samples are shown in Figure 2. The values for the aggregated samples can be reasonably represented by two straight lines.

The average dimensions obtained by light scattering, employing the Caufield-Ullman modification, and optical microscopy are compared in Table I. The point is that the particle dimensions of the more aggregated system can be semiquantitatively estimated by light-scattering

TABLE I
Diameters of Dow Latex Particles and Aggregates
from Light-Scattering and Optical Microscopy

	Particle diam., μ	
	Discrete system	Aggregated system
Nominal Size of Individual Particles from Electron Microscopy	1.8	1.8
Light-Scattering		
(a) high-angle slope and intercept	2.4	2.5
(b) initial slope and intercept	—	5.0
Optical Microscopy		
(a) aggregate diameter	2.1	3.3
(b) aggregate diameter >10 particles only	—	7.2

studies. This result arises from the fact that light scattering is sensitive to different sizes at different angular ranges.

Filled Silicone Rubber

A plot of $(x/I_\theta)^{1/2}$ versus x is shown in Figure 3. Values of $(x/I_\theta)^{1/2}_{x=0}$ versus $4 \sin^{1/2} (\theta/2)$ are illustrated in Figure 4. All such plots for HiSil, TK, and Quso resulted in data that could be represented by two straight lines intersecting at values of $4 \sin^2 (\theta/2) = 2$–3×10^{-2}. Equivalent sphere diameters calculated employing the Caufield-Ullman modification are summarized in Table II.

Since the diameters obtained via light scattering were two orders of magnitude larger than the dimensions of the individual primary filler particles as seen by electron microscopy (see Fig. 5) and the scattering diagram complex, some type of aggregation seemed likely.

TABLE II
Equivalent Sphere Diameters Calculated from the Caulfield-Ullman
Modification At Zero Sample Thickness

	Diameter, μ	
	High angle	Low angle
HiSil, vol-%		
2.2	2.4	7.3
7.5	2.6	5.9
9.8	2.5	4.1
15.5	1.8	7.3
TK, vol-%		
2.2	1.6	6.1
7.5	1.6	7.2
15.5	2.9	5.8
Quso, vol-%		
15.5	1.2	2.8

The resulting optical micrographs are illustrated in Figure 6 for a series of filler concentrations. The particles visible through optical microscopy appear to have a complex hierarchy of agglomeration. The smallest particles visible averaged about 5 μ in diameter and appeared roughly
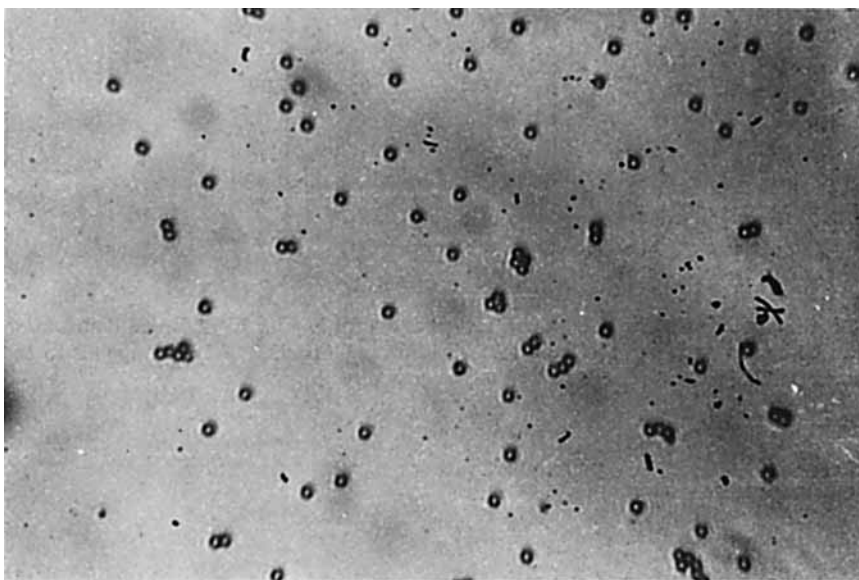
(a)
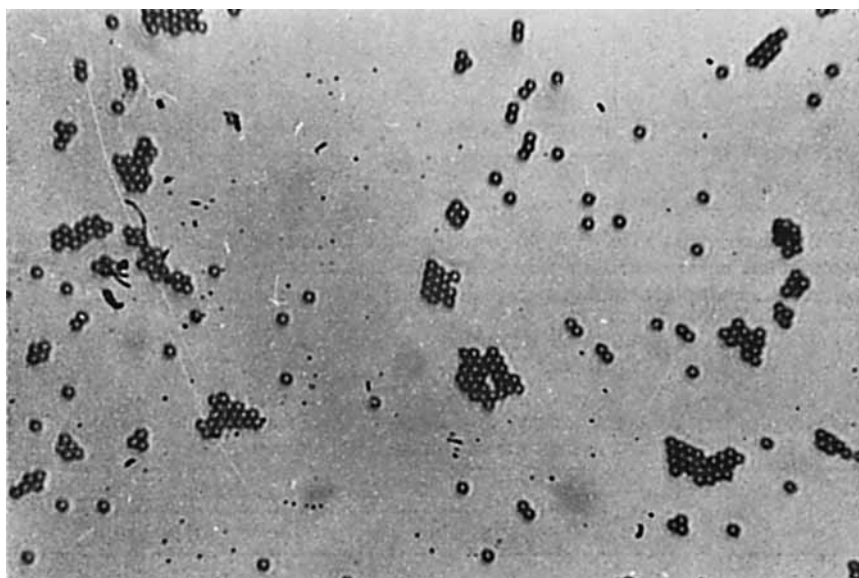
(b)

Fig. 1. Polystyrene latices dispersed in silicone gum: (a) well-dispersed system showing few aggregates; (b) aggregated system.
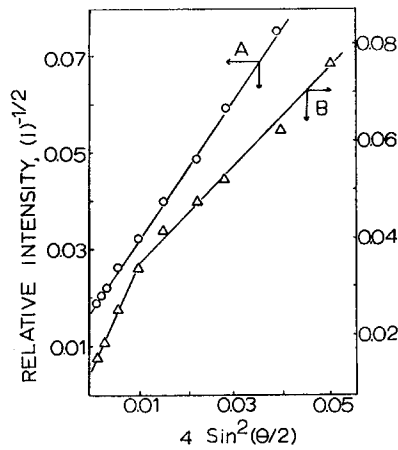
Fig. 2. Light-scattering results on materials shown in Fig. 1. A broad distribution can be interpreted from the B curve. The low angle portion of B corresponds to the larger particle sizes.
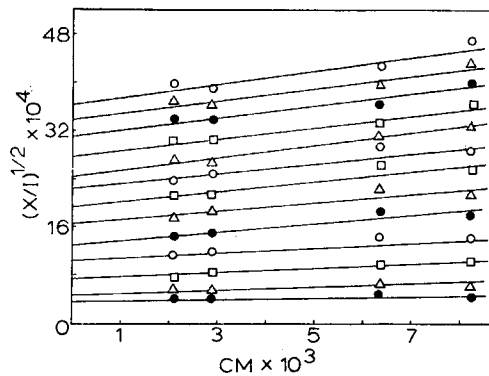

Fig. 3. Extrapolation of $(x/I_\theta)^{1/2}$ to zero sample thickness for 7.5 vol.-% TK. This is somewhat analogous to an extrapolation to zero concentration. The objective is to eliminate multiple scattering while maintaining the full concentration of filler.

TABLE III
Estimated Diameters of Agglomerates from Optical
Micrographs of Rubber-Filled Mixes

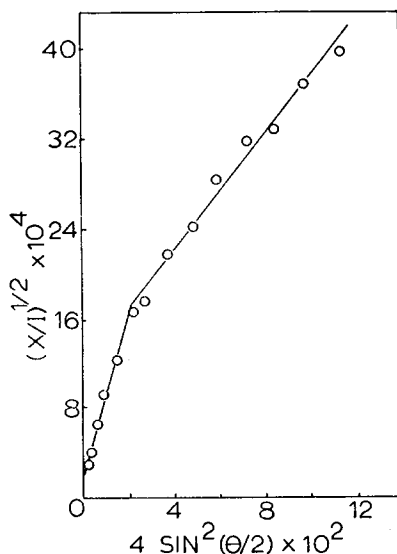|	Aggregate diam., μ	
	Primary	Secondary
HiSil	5–8	20–30
TK	<5	10–20
Quso	<3	5–10
Celite	3–5	3–5

Fig. 4. Angular distribution of scattered light for 15.5 vol-% HiSil dispersed in silicone gum. Graph is similar to that obtained on the aggregated material in Fig. 2 and suggests that the particle distribution of the filler is complex.

spherical. Some of these, in turn, appeared clustered together further to form secondary aggregates. This last phenomenon is most clearly illustrated in Figure 6b. The average sizes of the aggregates as measured from optical microscopy are summarized in Table III.

In connection with these experiments on silica filler morphology, a very curious discovery was made. The turbidity of the samples goes through a distinct maximum at about 7.5 vol-% filler. This finding, illustrated in Figure 7, employed data obtained from the fully cured materials. The TK and HiSil samples are distinctly more transparent to the eye at 15% filler than at 7.5% filler. The exact reason for this behavior remains unknown at the present time.

DISCUSSION

Light-scattering and optical microscopy studies on silica-reinforced silicone rubber suggest that the filler is dispersed with a very broad distribution of particle sizes. The primary particles are aggregated, and apparently the aggregates often appear clustered together to form larger agglomerates. This observation is not new. Some time ago Vold,[19] observing the highly caducous behavior of finely divided silicas suspended in chlorobenzene, had hypothesized a particle structure organized on three levels.

A corresponding state of agglomeration of reinforcing silica particles in organic elastomers also has been known for some time.[8,20] Through the somewhat artificial means of mixing dissolved silicones with reinforcing

silicas followed by film casting, Chahal and St. Pierre[21] recently showed
that agglomeration could be important in silicone elastomers. Up to
this time, however, agglomeration studies have been lacking whereby
reinforcing silicas were milled into silicone elastomers under conditions
approaching those employed industrially. While the data presented above
are only semiquantitative in the sense that exact agreement between mi-
croscopy and light scattering was lacking (and perhaps should not be ex-
pected), one must conclude that no theory of elastomer reinforcement can
be complete without inclusion of the agglomeration state in a natural
manner.

The important point is that these agglomerates do provide a logical
physical mechanism for internal energy dissipation during deformation.[1,2]
The large entropy change observed on elastomer deformation arises from
statistical changes in chain conformation. The complex agglomerate
structures contain many filler–filler interactions involving primary and
secondary chemical bonds in addition to elastomer chains. These chemical
bonds may be bent, stretched, or temporarily dissociated during deforma-
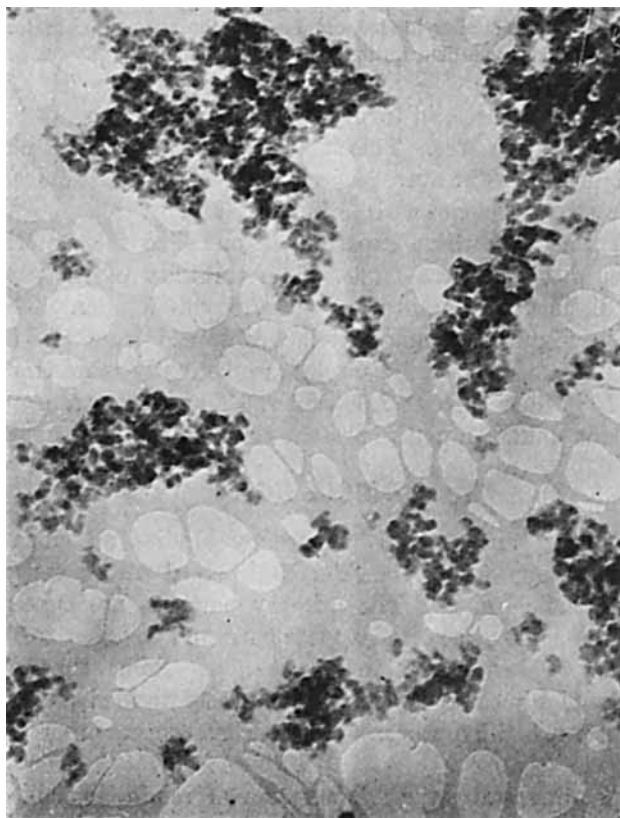

(a)

Fig. 5 (continued)

tion, giving rise to changes in internal energy and to an increased f_e/f ratio for the macroscopic body.

Because energetic as well as entropic modes of deformation are active, the modulus inside the filler agglomerates is variable and higher than the material as a whole. However, only relatively slight agglomerate deformations are required to produce large f_e/f ratios via the above mechanisms. A similar mechanism is thought to be active in the deformation of the plastic domains in self-reinforced ABA block copolymers.[22]

The appearance of two straight lines joined by well defined elbows in Figures 2 and 4 raised the possibility of interpreting these data in terms of weight- and number-average parameters. The theory, developed in 1954 by Benoit, Holtzer, and Doty[23] for random coils, was applied in a tentative manner to spheres in 1960 by Sperling and Easterwood.[24]

Two aspects of the present experiment need special consideration:

1.   Figures 2 and 4 are plots of $(1/I)^{1/2}$ versus $\sin^2(\theta/2)$. The theory of Benoit and co-workers[23] calls for plots of $1/I$ versus $\sin^2(\theta/2)$.
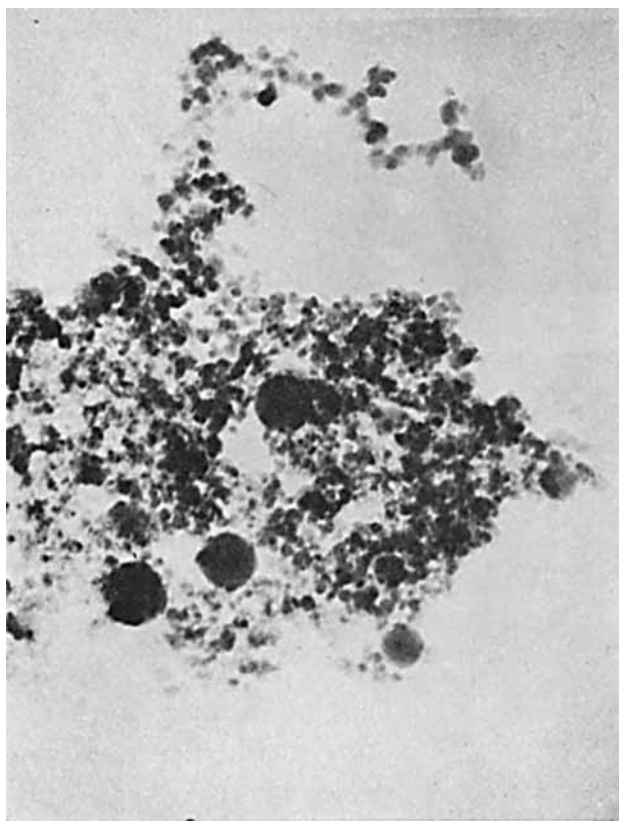

(b)

Fig. 5. Electron micrographs of (a) HiSil at 55,000×; (b) TK at 55,000×.

2.　All data were taken at finite filler levels, as permitted by the Debye surface area treatment.　The theory calls for extrapolation to zero concentration.　The extrapolation to zero sample thickness in Figure 3 to eliminate multiple scattering effects, of course, does not separate the particles.

Notwithstanding the above, if the reader wishes to interpret the high-angle data in Tables I and II in terms of a number-average diameter D_n,
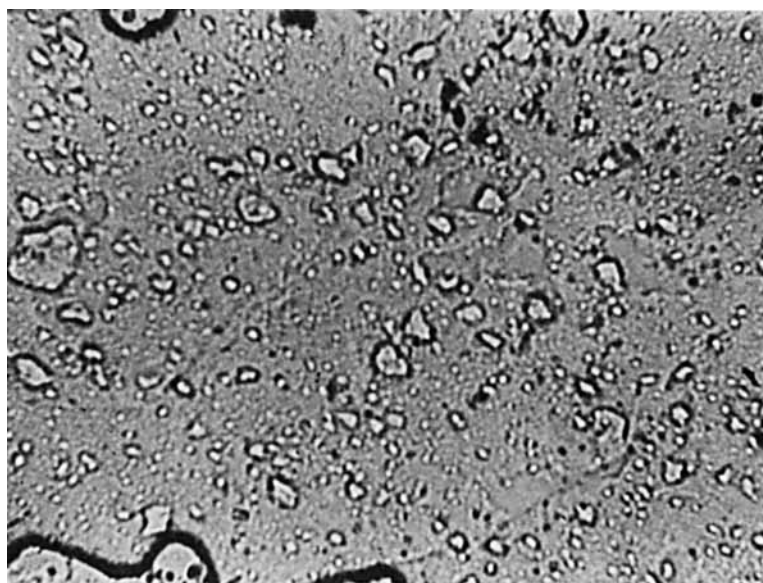

(a)

(b)

Fig. 5 (continued)

(c)
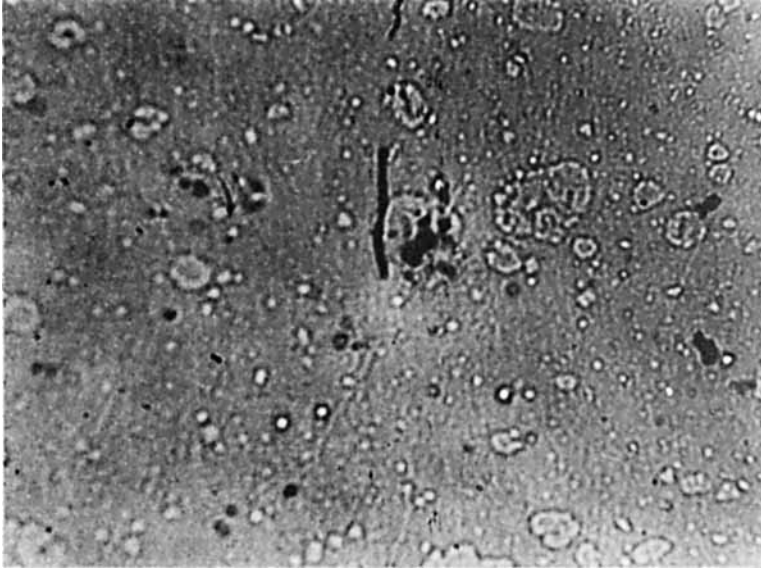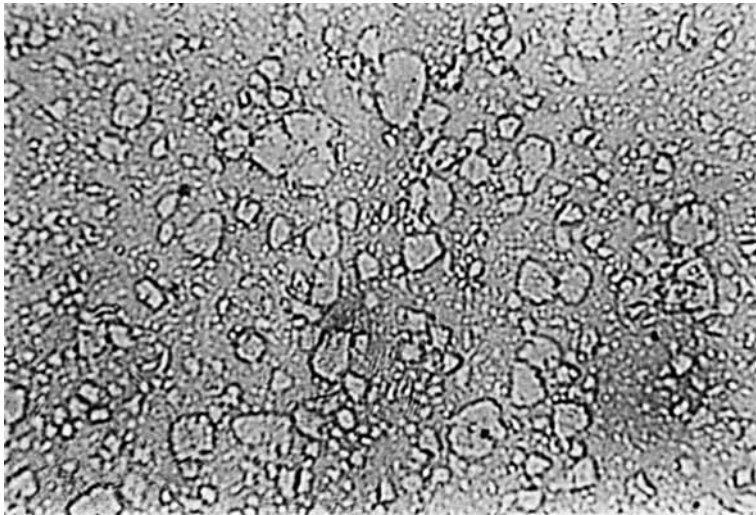
Fig. 6. HiSil-filled silicone rubber at (a) 2.4 vol-%; (b) 7.5 vol-%; (c) 15.5 vol-%. Magnification 100×. A broad particle distribution can be seen. This is clearest in (b), where the smaller particles retain their identity in the second level of agglomeration.

division of the listed results by $3^{1/2}$ conceivably has some meaning. If so, the data in Table II would be interpreted as having a particle distribution of D_w to D_n ratios in the range of 7 to 1.
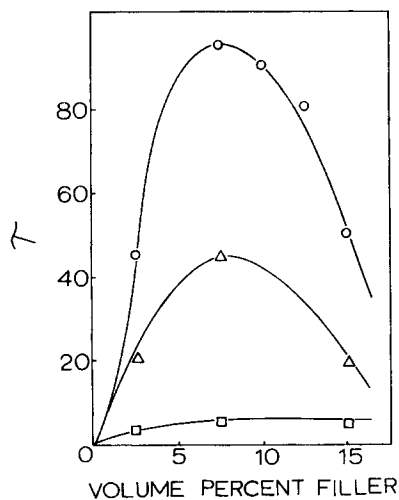

Fig. 7. Variation of turbidity τ with filler concentration in cured silicone elastomers. The clear maximum obtained for HiSil and TK is not well understood: (O) HiSil; (△) TK; (□) Quso.

References

1. A. V. Galanti and L. H. Sperling, *Polymer Letters*, **8**, 115 (1970).
2. A. V. Galanti and L. H. Sperling, *Polym. Eng. Sci.*, **10**, 177 (1970).
3. A. M. Gessler, *Rubber Chem. Technol.*, **42**, 850, 858 (1969).
4. R. J. Roe, D. D. Davis, and T. K. Kwei, to be presented at the American Physical Soc. Meeting, Dallas, Texas, March 1970.
5. S. Brunauer, P. H. Emmett, and E. Teller, *J. Amer. Chem. Soc.*, **60**, 309 (1938).
6. J. H. Bachmann, J. W. Sellers, M. P. Wagner, and R. W. Wolp, *Rubber Chem. Technol.*, **32**, 1286 (1959).
7. F. Bueche, in *Reinforcement of Elastomers*, Chap. 1, G. Kraus, Ed., Interscience, New York, 1965.
8. J. W. Sellers and F. E. Toonder, *ibid.*, Chap. 13.
9. M. P. Wagner and J. W. Sellers, *Ind. Eng. Chem.*, **51**, 961 (1959).
10. P. Debye and A. M. Bueche, *J. Appl. Phys.*, **20**, 518 (1949).
11. P. Debye, H. R. Anderson, Jr., and H. Brumberger, *J. Appl. Phys.*, **28**, 679 (1957).
12. E. Beebe and R. H. Marchessault, *J. Appl. Phys.*, **35**, 3182 (1964).
13. E. Beebe, R. L. Coalson, and R. H. Marchessault, *J. Polym. Sci.*, **13c**, 103 (1966).
14. L. H. Sperling, *J. Appl. Polym. Sci.*, **7**, 1891 (1963).
15. D. Caulfield and R. Ullman, *J. Appl. Phys.*, **33**, 1737 (1962).
16. D. Caulfield, Yung-Fang Yao, and R. Ullman, in *X-ray and Electron Methods of Analysis*, Chap. 7, H. van Olphen and W. Parrish, Eds., Plenum Press, New York, 1968.
17. K. A. Stacy, Light-Scattering in Physical Chemistry, Academic Press, New York, 1956, Chaps. 1 and 2.
18. F. A. Jenkins and H. E. White, Fundamentals of Optics, McGraw Hill, New York, 1957.
19. M. J. Vold, *J. Colloid Sci.*, **18**, 684 (1963).
20. N. G. Bartung, R. H. Fear, and M. P. Wagner, *Rubber Age*, **96**, 405 (1964).
21. R. S. Chahal and L. E. St. Pierre, *Macromolecules*, **2**, 193 (1969).
22. T. L. Smith, *Polymer Preprints*, **10**, 670 (1969).
23. H. Benoit, A. M. Holtzer, and P. Doty, *J. Phys. Chem.*, **58**, 635 (1954).
24. L. H. Sperling and M. Easterwood, *J. Appl. Polym. Sci.*, **4**, 25 (1960).